Science Advances
AAAS

Supplementary Materials for

Computation-driven redesign of an NRPS-like carboxylic acid reductase improves activity and selectivity

Kun Shi *et al.*

Corresponding author: Hui-Lei Yu, huileiyu@ecust.edu.cn

Sci. Adv. **10**, eadp6775 (2024)
DOI: 10.1126/sciadv.adp6775

This PDF file includes:

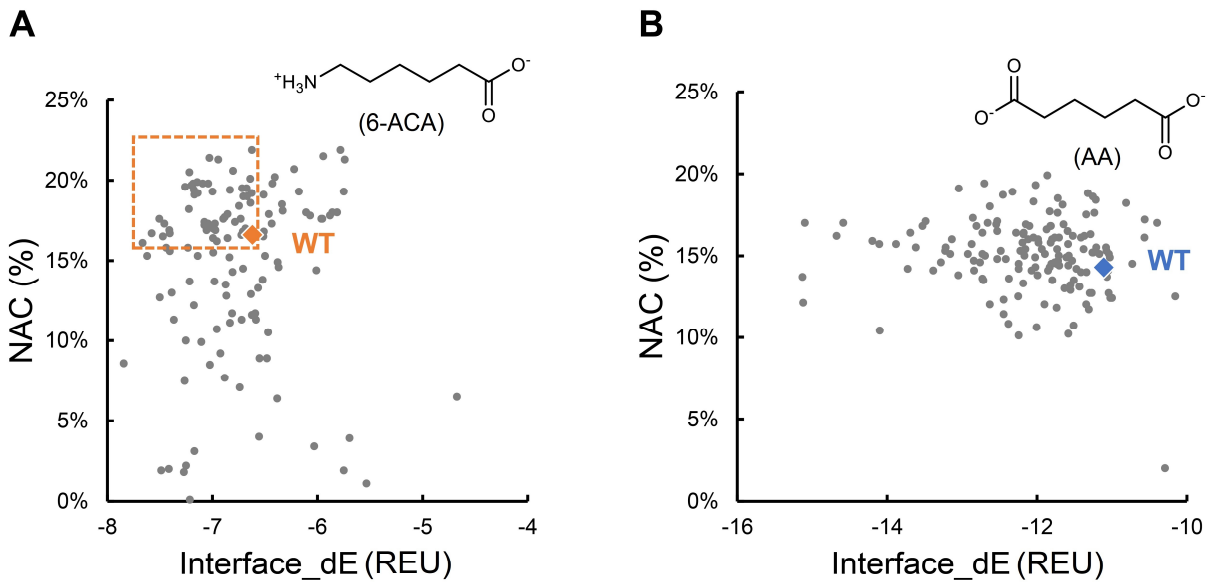

Fig. S1. ***In silico*** **site saturation mutagenesis.** (**A**) 6-ACA as substrate. Points in orange square: 38 mutants selected for experiment validation. (**B**) AA as substrate.

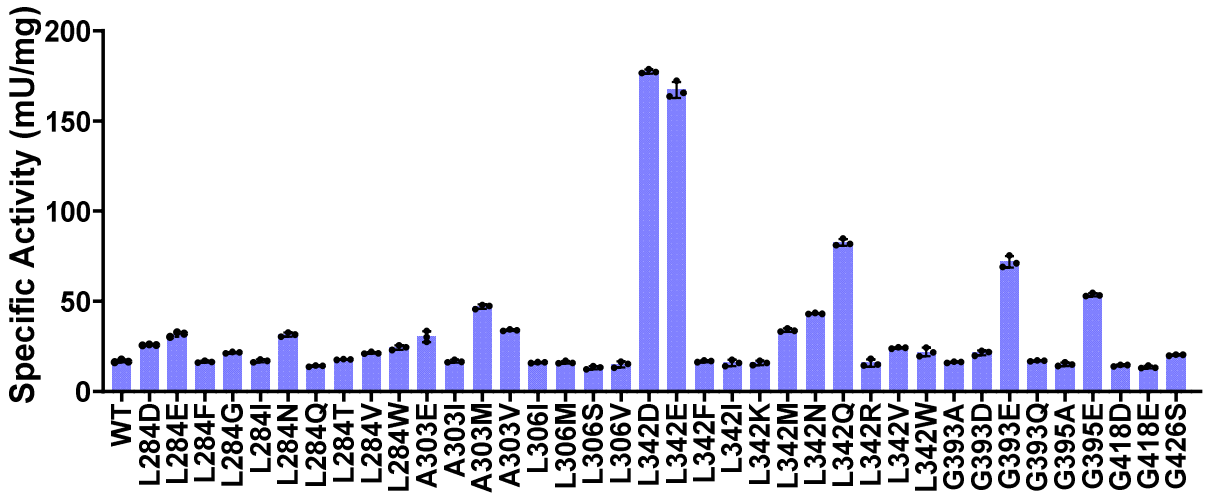

Fig. S2. Validation of *in silico* site mutations (selected from Fig. S1A) for reductase activity toward 6-ACA. Data are presented as mean values +/- SD (n=3 independent experiments). Assays were conducted with 10 mM substrates.

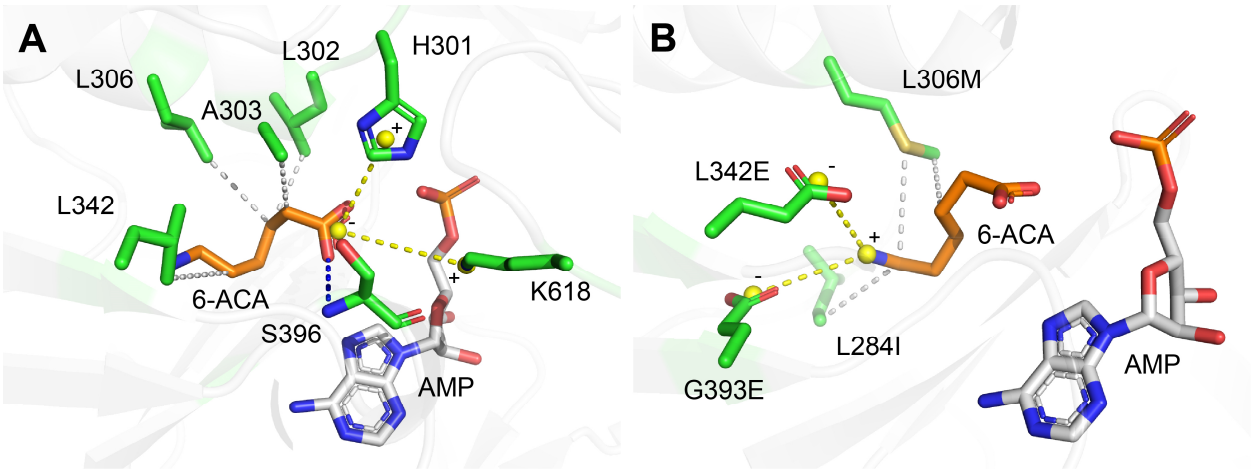

Fig. S3. Structural comparison of the Rosetta-predicted mode between the *Mab*CAR3_WT and ACA-4 with the bound substrate 6-ACA. (**A**) the active site of WT. (**B**) the active site of ACA-4, highlighting the predicted formation of new hydrophobic interactions and salt bridges. Yellow lines: salt bridge. Blue lines: hydrogen bond. Grey lines: hydrophobic interaction.

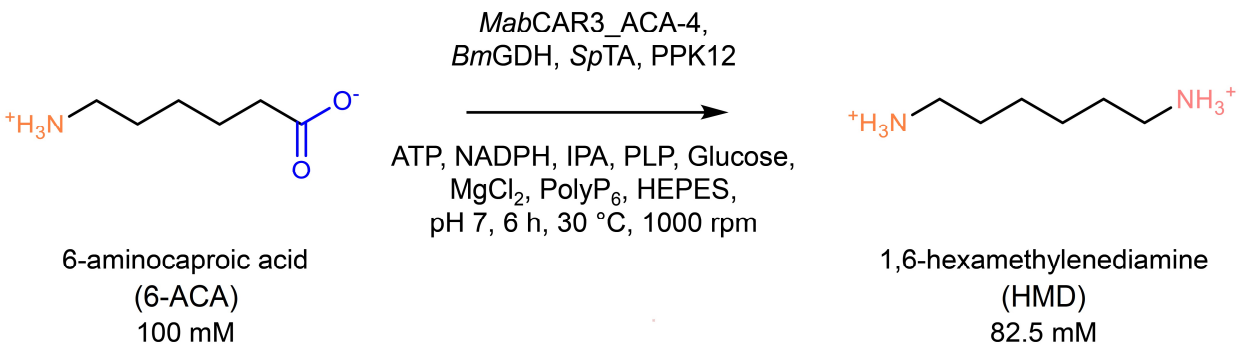

Fig. S4. The biosynthesis of HMD from 6-ACA using purified ACA-4 and other necessary enzymes.

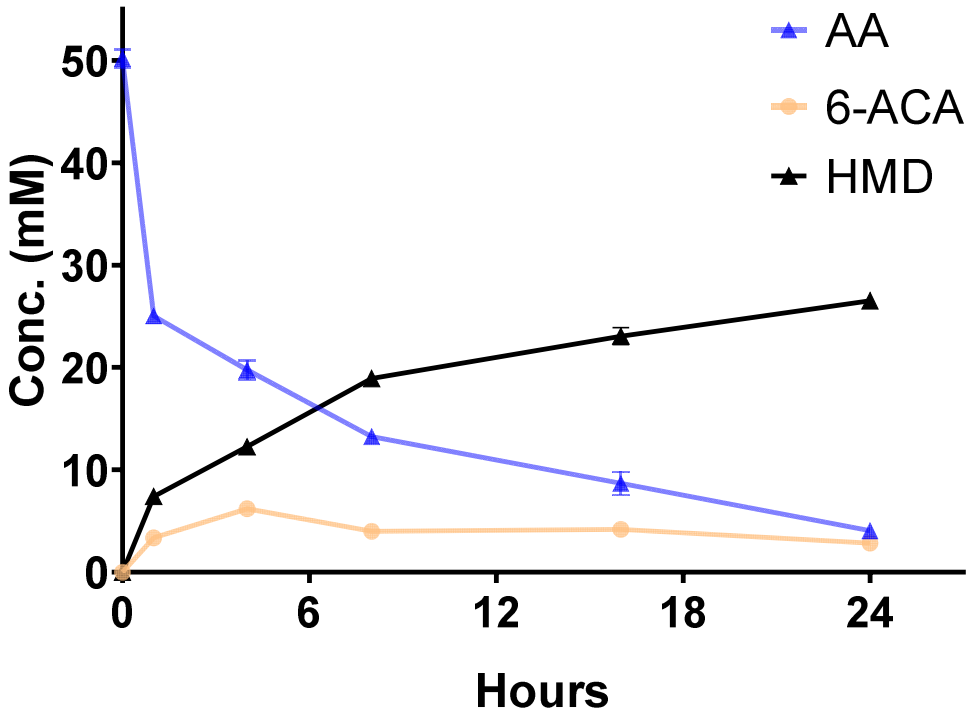

Fig. S5. Time course for condensed crude enzymes-catalyzed conversion of AA to HMD with 50 mM substrate in a 10-mL reaction mixture (using ACA-1 and ACA-4). Data are presented as mean values +/- SD (n=3 independent experiments). The reaction mixtures contained 500 mM HEPES-Na buffer (pH 7.5), 50 mM substrate AA, 1 mM $NADP^+$, 10 mM ATP, 120 mM $MgCl_2$, 120 mM Glucose, 1 mM PLP, 200 mM IPA, 100 mM $PolyP_6$; 8 mg/mL lyophilized enzyme powder of *Bm*GDH, 20 mg/mL lyophilized enzyme powder of PPK12, 50 mg/mL crude cell extract of *Mab*CAR3_ACA-1, 100 mg/mL crude cell extract of *Mab*CAR3_ACA-4, 240 mg/mL crude cell extract of *Sp*TA, 30 °C, 800 rpm.

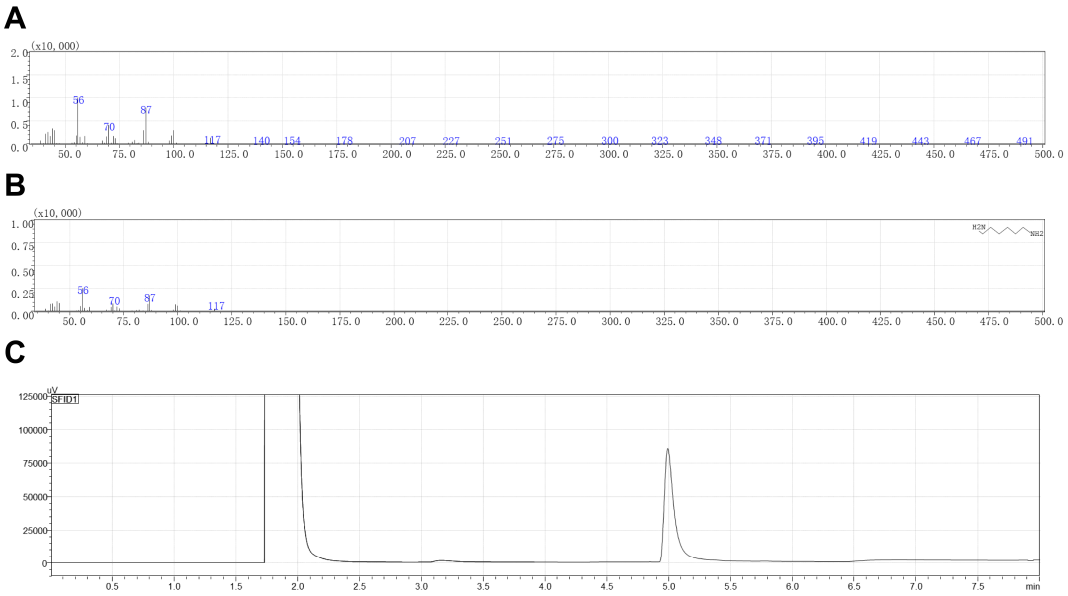

Fig. S6. The GC-MS/GC analysis of the preparation of HMD. (**A**) Mass spectrometry analysis of HMD product. (**B**) Mass spectrometry analysis of HMD standard in NIST database. (**C**) The GC results for the preparation of HMD (5 min).

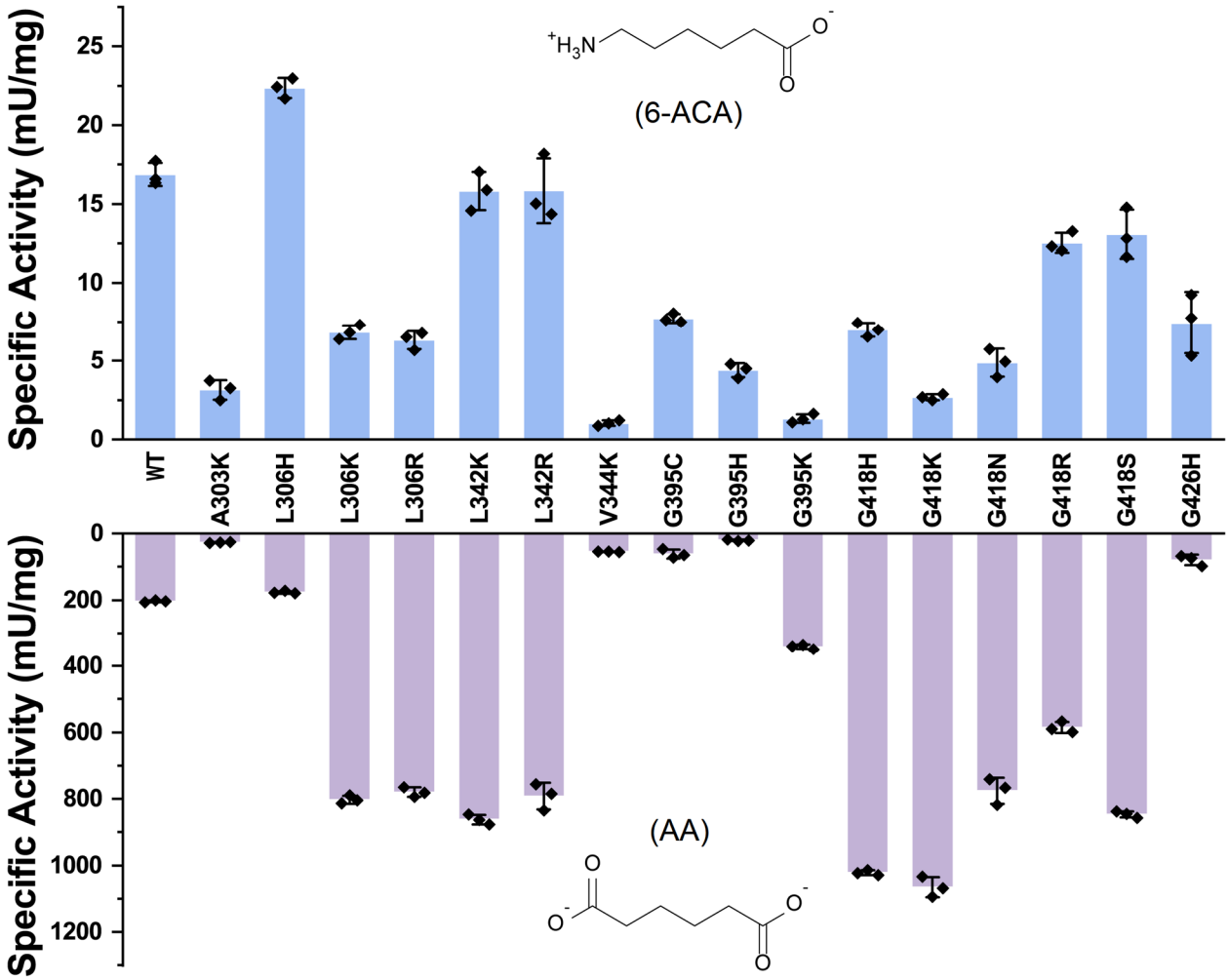

Fig. S7. The deamination activity of the 16 designs towards 6-ACA and AA. Data are presented as mean values +/- SD (n=3 independent experiments). Assays were conducted with 10 mM substrates.

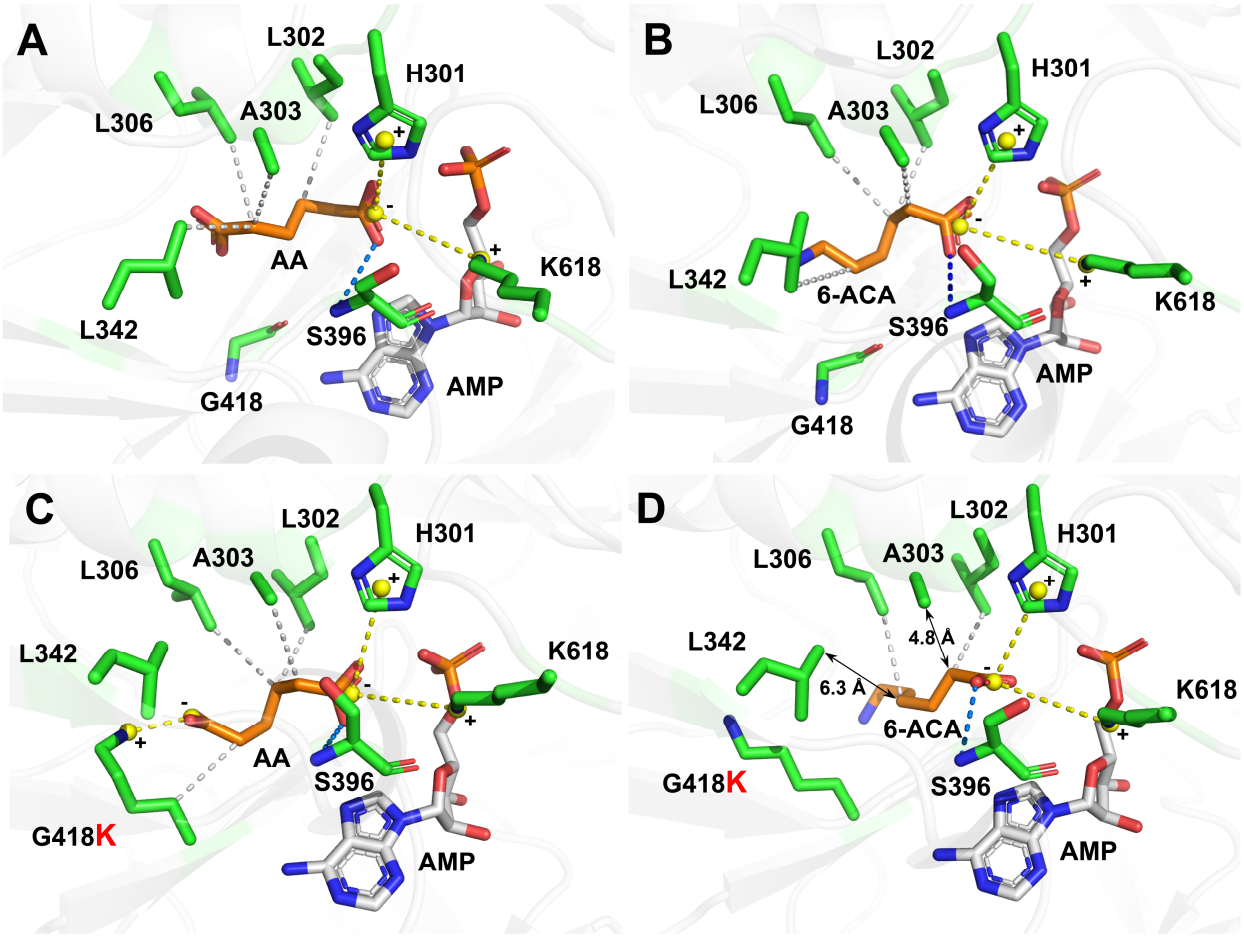

Fig. S8. Structural comparison of the Rosetta-predicted mode between the *Mab*CAR3_WT and G418K with the bound substrate 6-ACA and AA. (**A**) WT bound AA. (**B**) WT bound 6-ACA. (**C**) G418K bound AA. (**D**) G418K bound 6-ACA. Grey lines: hydrophobic interaction. Orange lines: salt bridge. Blue lines: hydrogen bond.

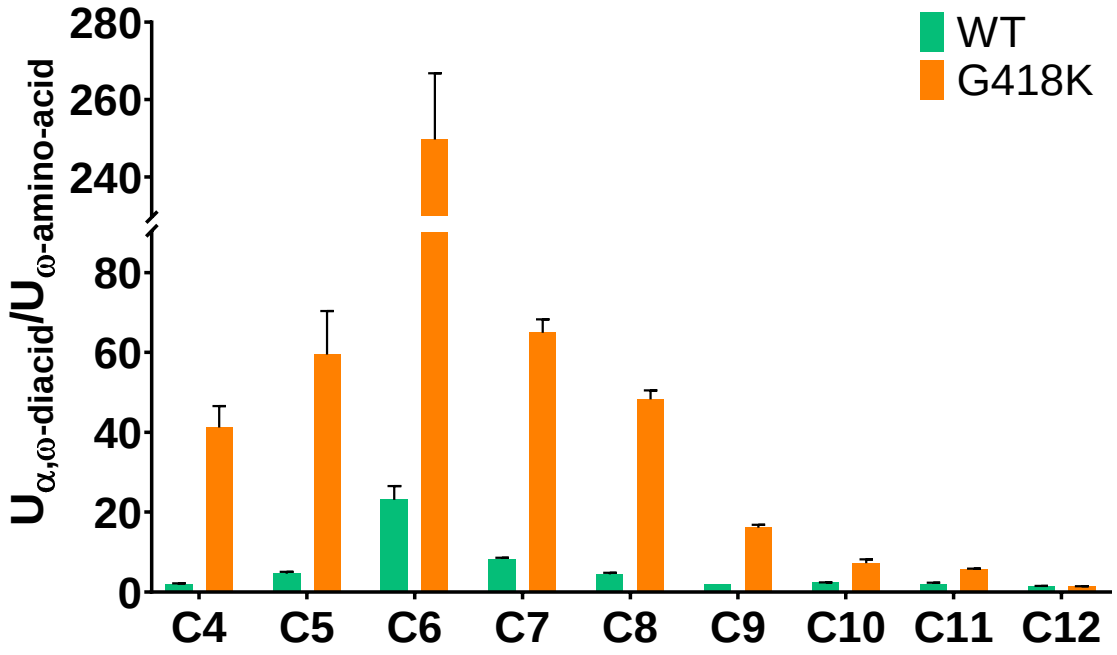

Fig. S9. $U_{\alpha,\omega\text{-diacid}}/U_{\omega\text{-amino-acid}}$ of G418K compared with wildtype (WT). Assays were conducted with 5 mM substrates. Error bars reflect the standard deviations from three replicates.

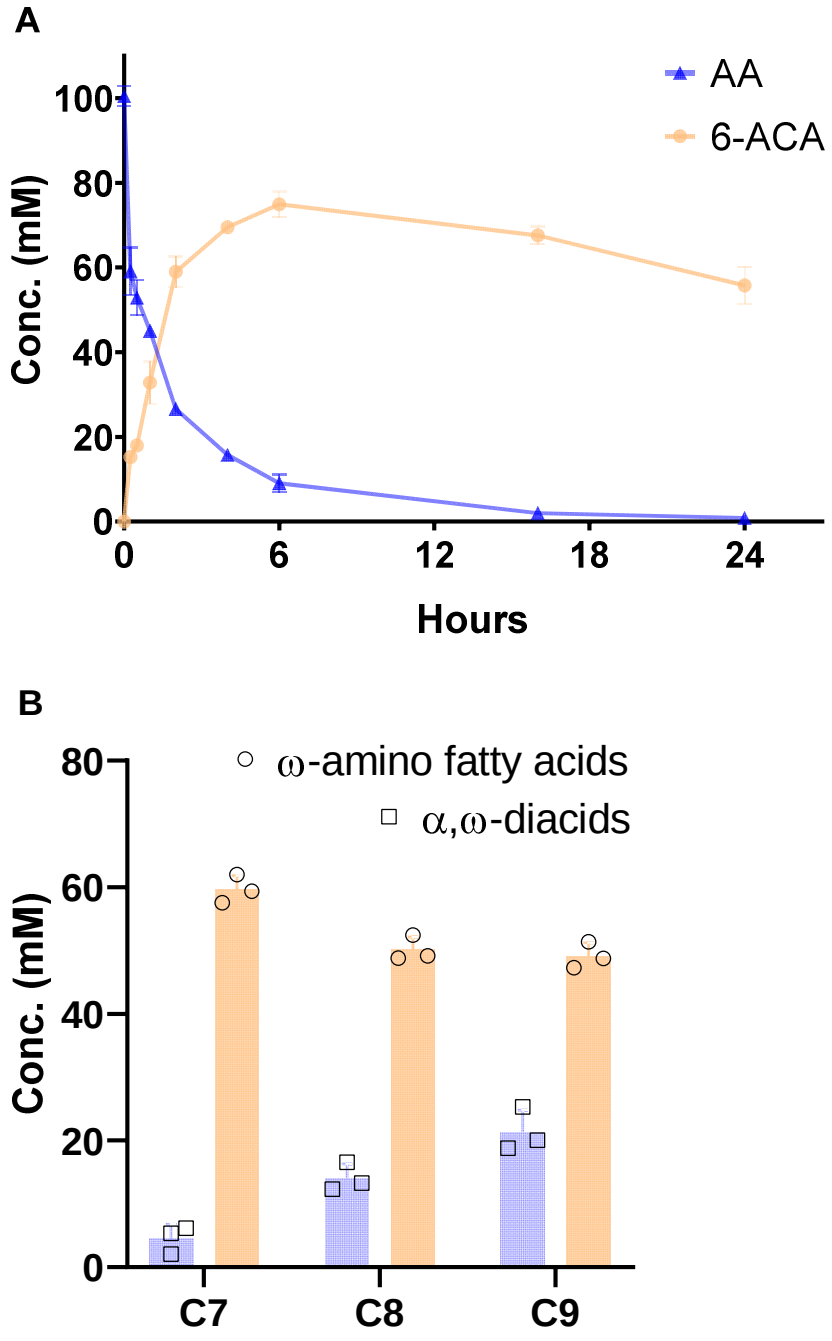

Fig. S10. Exploring substrate scope of a refined biocatalytic system (10 mL) for synthesizing various ω-amino fatty acids (C6-C9). (**A**) Reaction time-course for 6-ACA biosynthesis with crude enzymes. (**B**) Conversion of α,ω-diacids (C7-C9) to corresponding ω-amino fatty acids using crude *Mab*CAR3_G418K and other necessary enzymes (6 h). Data are presented as mean values +/- SD (n=3 independent experiments).

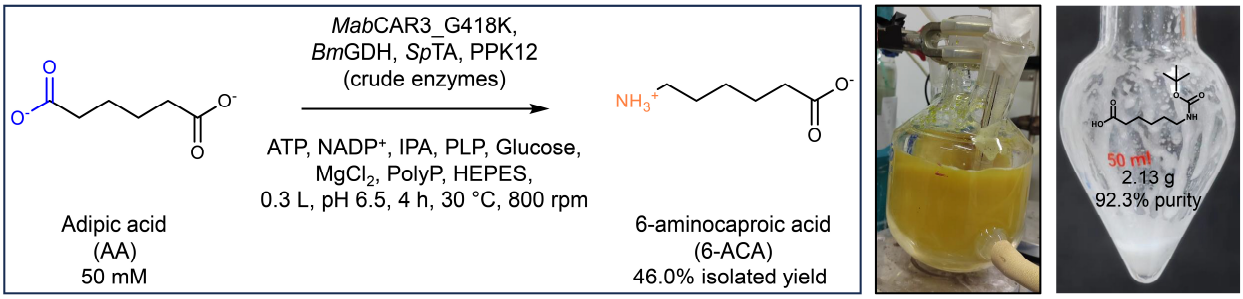

Fig. S11. Synthesis of 6-ACA derivative at the gram scale. Data are from one independent experiment.

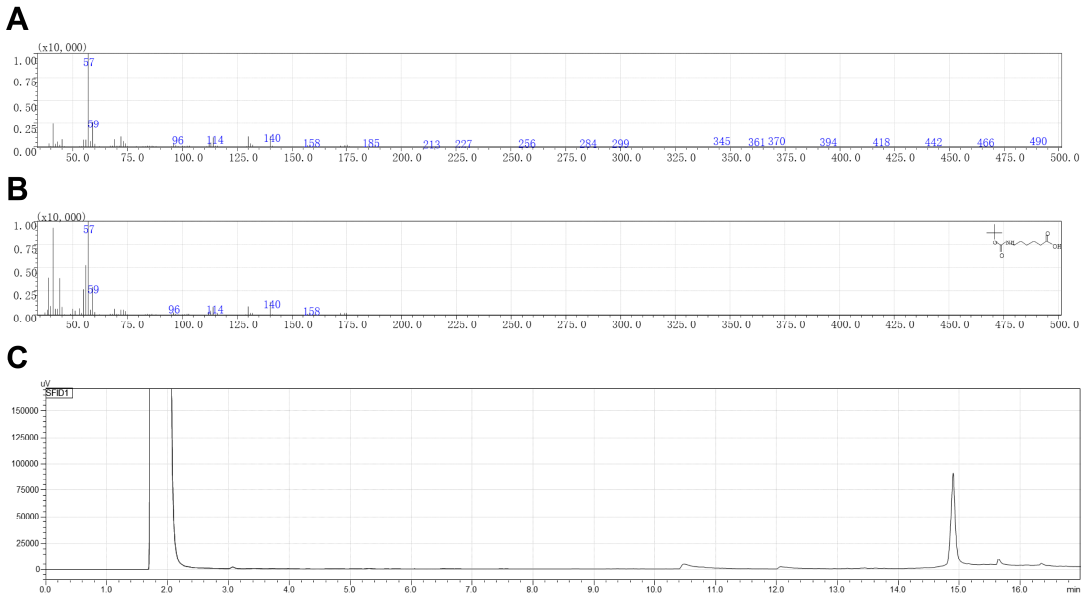

Fig. S12. The GC-MS/GC analysis of the preparation of Boc-ε-Ahx-OH. (**A**) Mass spectrometry analysis of Boc-ε-Ahx-OH product. (**B**) Mass spectrometry analysis of Boc-ε-Ahx-OH standard in NIST database. (**C**) The GC results for the preparation of Boc-ε-Ahx-OH (14.9 min).

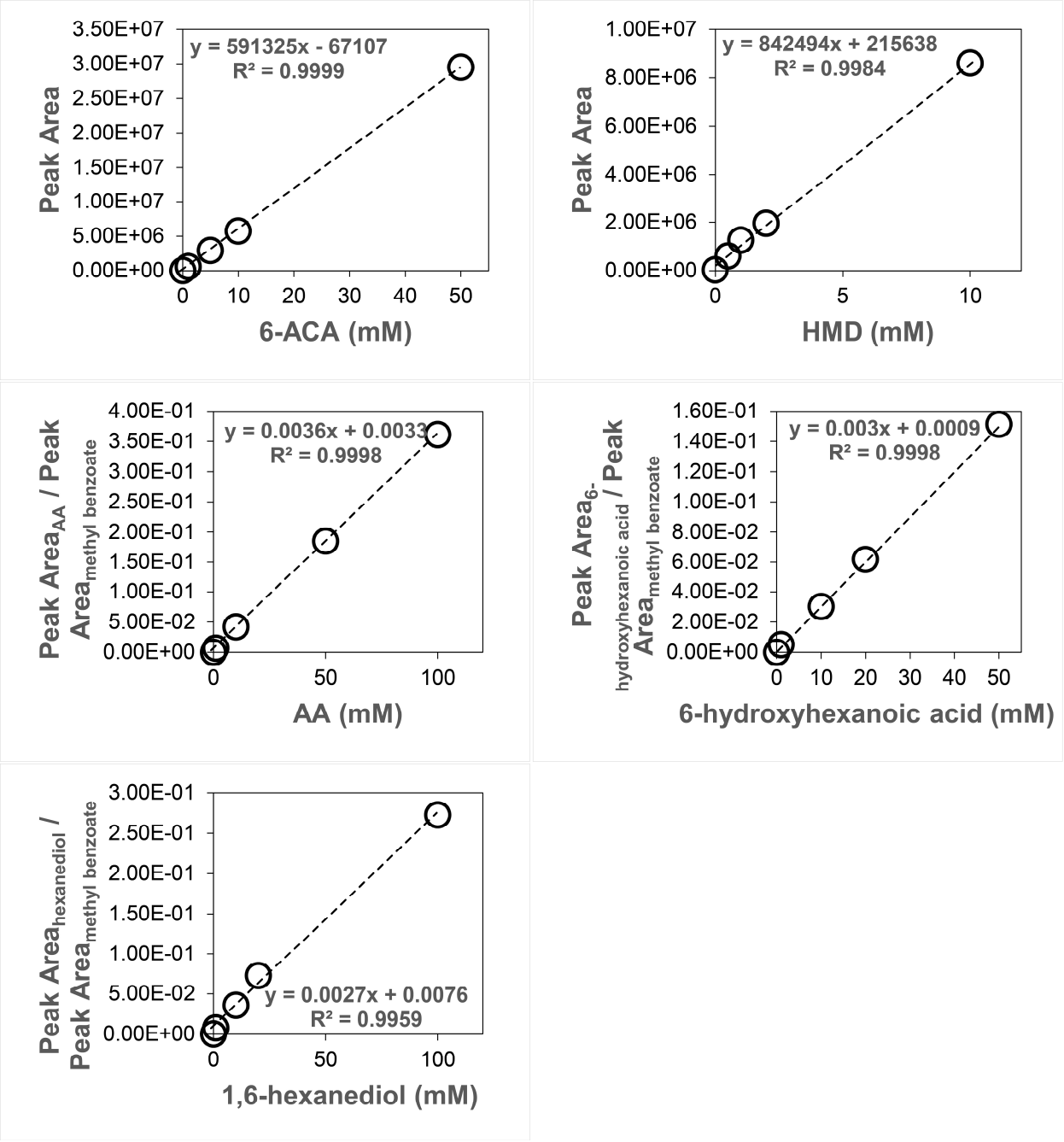

Fig. S13. Calibration curves for product and intermediate.

Table S1. Rosetta score (interface_dE) and NAC frequency of selected mutants from Fig. S1A.

CARs	interface_dE	NAC frequency
WT	-6.62	16.6%
L284D	-7.58	16.7%
L284E	-7.41	16.9%
L284F	-7.08	17.2%
L284G	-7.22	18.2%
L284I	-7.06	16.9%
L284N	-7.47	16.5%
L284Q	-7.66	16.1%
L284T	-7.23	15.8%
L284V	-7.14	15.3%
L284W	-7.08	17.4%
A303E	-7.17	19.1%
A303I	-7.04	17.3%
A303M	-7.41	16.7%
A303V	-7.46	17.3%
L306I	-7.20	19.7%
L306M	-6.97	16.9%
L306S	-7.09	19.8%
L306V	-7.22	20.5%
L342D	-7.62	15.3%
L342E	-7.26	19.6%
L342F	-6.99	17.0%
L342I	-7.00	19.3%
L342K	-6.96	16.2%
L342M	-7.03	21.4%
L342N	-7.51	17.6%
L342Q	-7.14	19.9%
L342R	-7.44	15.8%
L342V	-6.90	17.6%
L342W	-6.88	17.7%
G393A	-6.99	16.4%
G393D	-7.04	19.8%
G393E	-7.14	19.2%
G393Q	-7.18	19.8%
G395A	-7.41	15.6%
G395E	-7.17	19.4%
G418D	-6.99	15.5%
G418E	-6.98	17.3%
G426S	-6.94	21.3%

Table S2. Candidate residues in the combinatorial mutation library.

Position	Residue	Number of residues
284	W V T Q N E D G F I L	11
303	A V M I	4
306	L I M	3
342	E D	2
393	E G D Q A	5
418	G E D	3
426	S G	2
*Total 7920 mutants in the library.		

Table S3. Combinatorial mutations selected for experiment characterization.

Name	Combinatorial mutations
ACA-1	284D303M306I342E393A
ACA-2	284D306M342E
ACA-3	284D303I306I342E418D
ACA-4	284I306M342E393E
ACA-5	284D306M342E393A418E
ACA-6	284D306M342E393E
ACA-7	284E306M342E393A426S
ACA-8	284F306I342D393E
ACA-9	284F306M342D393E
ACA-10	303M306I342D393E
ACA-11	303M306M342D393Q
ACA-12	284D306M342D393E
ACA-13	306I342D418D
ACA-14	284E303I306I342E393E
ACA-15	284D303M306I342E393A418D
ACA-16	284Q306M342E418E426S
ACA-17	284D303I306I342D393E418E
ACA-18	284F306I342E393Q

*WT: 284L/303A/306L/342L/393G/418G

Table S4. Fold changes in specific activity of the *Mab*CAR3 mutants compared to the wild type with different substrates.

Substrates	U_{ACA-1}/U_{WT}	U_{ACA-4}/U_{WT}
butanedioic acid	7.23	10.9
4-aminobutyric acid	0.77	1.10
glutaric acid	6.59	1.86
5-aminovaleric acid	4.00	4.51
AA	10.3	1.76
6-ACA	28.1	37.6
pimelic acid	3.55	0.92
7-aminoheptanoic acid	10.8	32.4
octanedioic acid	3.79	1.08
8-aminocaprylic acid	6.40	12.6
azelaic acid	3.02	1.36
9-aminononanoic acid	1.83	4.16
sebacic acid	1.93	1.58
10-aminodecanoic acid	1.70	3.63
undecandioic acid	3.54	1.57
11-aminoundecanoic acid	0.81	1.68
dodecanedioic acid	2.01	1.55
12-aminododecanoic acid	1.22	1.98

Assays were conducted with 5 mM substrates.

Table S5. Rosetta score (interface_dE) and NAC frequency of selected mutants from Fig. 7A.

CARs	AA		6-ACA	
	interface_dE	NAC (%)	interface_dE	NAC (%)
WT	-11.07	15.3	-6.62	16.6
A303K	-13.53	16.8	-6.47	10.5
G418S	-13.23	15.3	-6.81	14.3
G418K	-12.68	16.3	-6.37	14.6
L342R	-13.88	15.7	-7.44	15.8
L342K	-14.67	16.2	-6.96	16.2
G395H	-13.13	16.0	-6.63	11.6
G426H	-13.69	16.4	-5.95	21.5
V344K	-14.58	17.0	-6.52	13.8
G418R	-12.76	14.6	-6.44	17.3
L306H	-12.63	18.0	-6.83	11.1
L306K	-12.92	15.1	-6.50	15.3
L306R	-12.81	16.8	-6.56	13.3
G395C	-12.12	16.0	-6.11	18.0
G395K	-15.13	13.7	-6.59	11.3
G418N	-12.10	16.8	-6.87	13.5
G418H	-11.34	17.5	-6.59	11.7

Table S6. The biosynthesis of HMD from 6-ACA using different CARs (WT, ACA-1 and ACA-4) and other necessary enzymes.

CARs	HMD (mM)
WT	1.4 ± 0.3
ACA-1	19.9 ± 0.9
ACA-4	22.8 ± 1.1

Reaction mixtures (200 μL) contained 100 mM HEPES-Na buffer (pH 7.5), 50 mM substrate 6-ACA, 1 mM NAD(P)H, 10 mM ATP, 60 mM $MgCl_2$, 60 mM Glucose, 0.5 mM PLP, 100 mM IPA, 50 mM PolyP, 20 μg of *Bm*GDH, 80 μg of PPK12, 146 μg of CARs, 180 μg of *Sp*TA, 30 °C, 1000 rpm, 18 h. Data are presented as mean values +/- SD (n=3 independent experiments).

Table S7. Enzymes (wild-type) used in this work.

Enzyme	Organism	Uniprot ID	Plasmid	Cloning site	Mass
*Mab*CAR3	*Mycobacterium abscessus*	A0A1M9KYS5	pET-30b	NdeI/XhoI	129 kDa
*Sp*TA	*Silicibacter pomeroyi*	Q5LMU1	pETDuet-1	NdeI/XhoI	51 kDa
PPK12	*Erysipelotrichaceae bacterium*	A0A3D5XRJ5	pET-28a	NdeI/XhoI	36 kDa
*Bs*Sfp	*Bacillus subtilis*	P39135	pCDFDuet-1	BamHI/NotI	26 kDa
*Bm*GDH	*Bacillus megaterium*	P40288	pET-28a	BamHI/HindIII	28 kDa